# Chapter 17
# An Orthogonal View of the Polyreference Least-Squares Complex Frequency Modal Parameter Estimation Algorithm

**William Fladung and Håvard Vold**

**Abstract** The polyreference least-squares complex frequency (PLSCF) modal parameter estimation algorithm has gained some popularity since the introduction of its single-reference predecessor shortly after the turn of this millennium. It is a z-domain (i.e., discrete time) method that uses a complex exponential frequency mapping from the imaginary frequency axis to the unit circle on the complex plane. While it operates directly on frequency response functions, this method has been interpreted to be essentially equivalent to the polyreference time-domain algorithm, with the application of the discrete Fourier transform implicit in its formulation. Another way to view this algorithm is that its basis functions are a set of orthogonal polynomials evaluated around the unit circle. This paper shows that the PLSCF method can be implemented as an orthogonal polynomial algorithm by a simple substitution of the basis functions. Furthermore, the PLSCF method is extended for applicability to uneven frequency spacing by generating the z-domain basis functions with the same procedure that is used for the traditional Laplace-domain orthogonal polynomials. The paper also illustrates how PLSCF, the orthogonal polynomial algorithm, and their ancestor the rational fraction polynomial method all start from the same place but move to different neighborhoods to do their work.

**Keywords** Modal parameter estimation • Orthogonal polynomial • Complex frequency

## 17.1 Introduction

The rational fraction polynomial (RPF) [1] algorithm is the entry-level model of the high-order, frequency-domain modal parameter estimation methods. However, it has some well-known issues with numerical ill-conditioning for a high model order and a wide frequency range. The remedies for this shortcoming have been frequency mapping and a change of basis functions. The traditional, Laplace-domain orthogonal polynomial (LDOP) [2][1] algorithm scales and rotates the solution space from the frequency range on the imaginary axis to the interval of $-1$ to $+1$ on the real axis and substitutes orthogonal polynomials for the power polynomials. The polyreference least-squares complex frequency (PLSCF) algorithm uses a different frequency mapping and basis functions to address the numerical ill-conditioning.

## 17.2 One View of PLSCF

PLSCF is based on a z-domain model, where the z-domain is to the discrete time domain as the Laplace domain is to the continuous time domain. In the published works on the algorithm [3–6], the reduced normal equations are derived for the linear least-squares solution for the coefficients of the numerator and denominator polynomials of the rational fraction polynomial model of the frequency response function (FRF). The polynomial coefficients are assumed to be real-valued, which is enforced by including the conjugate FRF at the negative frequencies. A discrete time-domain model for complex trigonometric basis functions of the form $e^{jk\omega\Delta t}$ is chosen for a fast implementation of the reduced normal equations that has better numerical conditioning than the continuous time power polynomials. This choice also imposes even frequency

[1] Fladung and Vold [2] is a companion piece to this paper and should be considered a prerequisite for much of the discussion herein.

W. Fladung (✉) • H. Vold
ATA Engineering, Inc., 13290 Evening Creek Drive South, Suite 250, San Diego, CA 92128, USA
e-mail: bfladung@ata-e.com



M. Mains (ed.), *Topics in Modal Analysis, Volume 10*, Conference Proceedings of the Society for Experimental Mechanics Series, DOI 10.1007/978-3-319-15251-6_17

spacing and produces terms in the reduced normal equations that are equivalent to the inverse discrete Fourier transform of the FRF. For a nontrivial solution of the reduced normal equations, it is proposed to normalize by the highest-order denominator polynomial coefficient. The solution is obtained by first eliminating the numerator variables and solving for the denominator coefficients from the condensed set of equations. In fact, only the denominator polynomial, which is the characteristic equation, is necessary to estimate the poles and modal participation factors from a standard companion matrix.

Because the application of the discrete Fourier transform essentially creates the impulse response functions (IRFs) in the reduced normal equations, PLSCF can be viewed as the frequency-domain equivalent of the polyreference time-domain (PTD) algorithm. Although PLSCF processes FRFs instead of IRFs, it is in essence a discrete time-domain algorithm and as such it is subject to aliasing because the frequencies of the z-domain poles, which must wrap around the unit circle on the complex plane, are then mapped back into the original frequency range. However, this choice of complex trigonometric basis functions does offer very favorable numerical conditioning behavior, and PLSCF can accommodate a wide frequency range containing many modes.

## 17.3 An Orthogonal View of PLSCF

Another way to view the PLSCF algorithm is in terms of frequency mapping and basis functions. The normalized frequency $\tilde{\omega}_i \in [-1, +1]$ on the imaginary axis is mapped to the unit circle on the complex plane with

$$z_i = e^{j\pi\tilde{\omega}_i}. \tag{17.1}$$

The positive frequency is mapped to the top half of the unit circle and the negative frequency is mapped to the bottom, as shown in Fig. 17.1.

The basis functions are $z^k$, which are polynomials of a complex variable given by the frequency mapping in Eq. 17.1. By Euler's formula, the complex exponentials $e^{j\pi k\tilde{\omega}}$ are real cosine functions and imaginary sine functions going around the unit circle, as shown in Fig. 17.2 for $k$ from zero to five.

These sine and cosine functions are periodic in the interval of $-\pi$ to $\pi$ and are also orthogonal over this interval. That is, the set of $z^k$ for $k = 0, 1, 2, \ldots$ is a set of orthogonal polynomials. In addition, this set of complex trigonometric basis functions has favorable attributes to address the numerical conditioning issues.

From this point of view, PLSCF can be thought of as a z-domain orthogonal polynomial (ZDOP) algorithm and can be implemented in the same manner as the LDOP algorithm – just with a different frequency mapping and set of basis functions. The numerator terms can be removed to greatly reduce the size of the least-squares problem, the correlation matrix can be accumulated response by response with QR decomposition, and the orthogonal complement can be used to get all possible

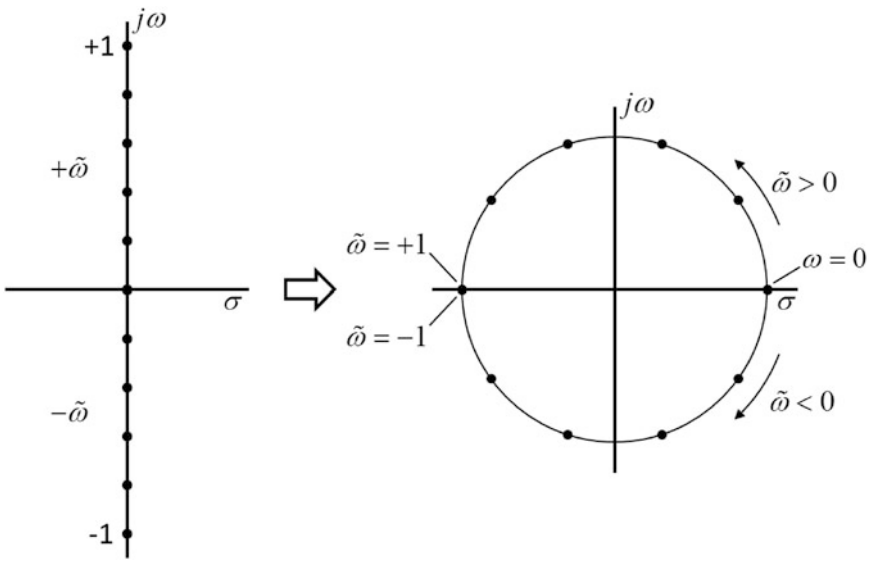


**Fig. 17.1** The complex frequency mapping for PLSCF

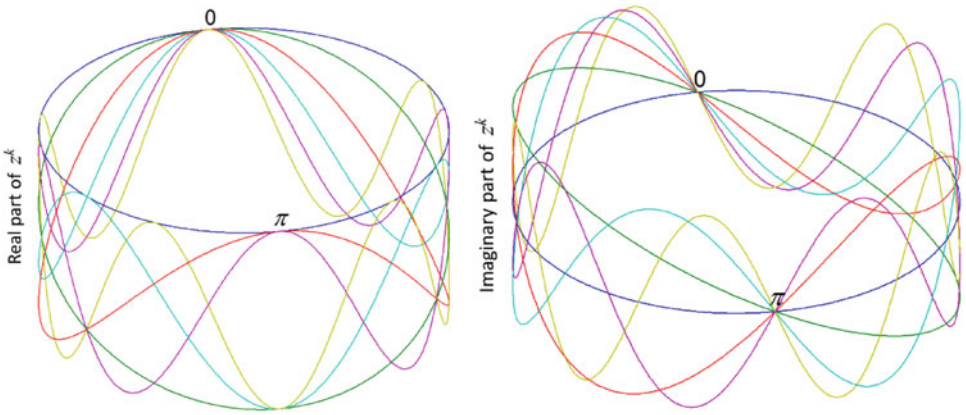


**Fig. 17.2** Z-domain basis functions, cosines as the real part (*left*) and sine as the imaginary part (*right*)

overdetermination with less effort. It's just a simple substitution of the z-domain orthogonal polynomials for the Laplace-domain orthogonal polynomials.

The z-domain orthogonal polynomials $\xi_k(z_i) = z_i^k$ for $k = 0, 1, \ldots, N_s$ are constructed recursively, with each successive polynomial being one order higher than the preceding. Here $N_s$ is the number of spectral lines, and the highest-order polynomial that can be defined for an interval containing $N_s$ data points is $N_s - 1$, since the lowest order is zero – but not nearly that many are needed when using the orthogonal complement. The zeroth-order basis function $\xi_0 = z^0$ is a real constant normalized to have unity length (i.e., a 2-norm of one). Then the higher orders are generated recursively as

$$\xi_k(z_i) = z_i^k = z_i \times z_i^{k-1} = z_i \xi_{k-1}(z_i) \quad \text{for } k \geq 1, \text{ where } z_i = e^{j\pi\tilde{\omega}_i}. \tag{17.2}$$

## 17.4 Frequency Mapping

The key to implementing PLSCF as an orthogonal polynomial algorithm is getting the frequency mapping just right. If the frequency range $f \in [f_{min}, \ f_{max}]$ is normalized by just dividing by $f_{max}$, the resulting $z^k$ basis function will not be orthogonal if $\{f\}\{min\}>0$ because the mapped interval must wrap all the way around the unit circle for the sines and cosines to be periodic. Rather, the frequency range must first be shifted to a baseband of $f' \in [0, \ f'_{max}]$, where $f'_{max} = f_{max} - f_{min}$. Then the shifted frequency range is scaled from $-1$ to 1, where the shifted and scaled interval of $\tilde{\omega} \in [-1, +1]$ can be mapped from the imaginary axis to the unit circle on the complex plane with Eq. 17.1, as shown in Fig. 17.3. There is one other small but important detail that must not be overlooked, which is that there cannot be coincident mapped points at 0 and $\pm\pi$, otherwise the sines and cosines will not be periodic. This means that the first and last spectral lines must be omitted when making the mirrored negative frequency.

The z-domain poles $z_r$ are mapped back to Laplace-domain poles $\tilde{\lambda}_r$ in the shifted and scaled interval of $[-1, +1]$ as

$$z_r = e^{\pi\tilde{\lambda}_r} \quad \rightarrow \quad \tilde{\lambda}_r = \frac{\ln(z_r)}{\pi}, \tag{17.3}$$

then rescaled to the shifted frequency range with $\lambda'_r = f'_{max}\tilde{\lambda}_r$, and finally shifted back to the original frequency range with $\lambda_r = \lambda'_r \pm j f_{min}$ by moving the imaginary parts of the conjugate poles in the right direction.

## 17.5 Companion Matrices

The other differences for the ZDOP algorithm are a simplification of the LDOP generalized eigenvalue problem to the "standard" companion matrix and replacing the Laplace-domain poles $\lambda_r$ with z-domain poles $z_r$. For the formulation that normalizes the characteristic equation with the highest-order coefficient $\alpha_m$ as an identity, the eigenvalue problem becomes

$$(C + Q)\,x = z_r W x \quad \rightarrow \quad (C + 0)\,x = z_r I x \quad \rightarrow \quad Cx = z_r x, \tag{17.4}$$

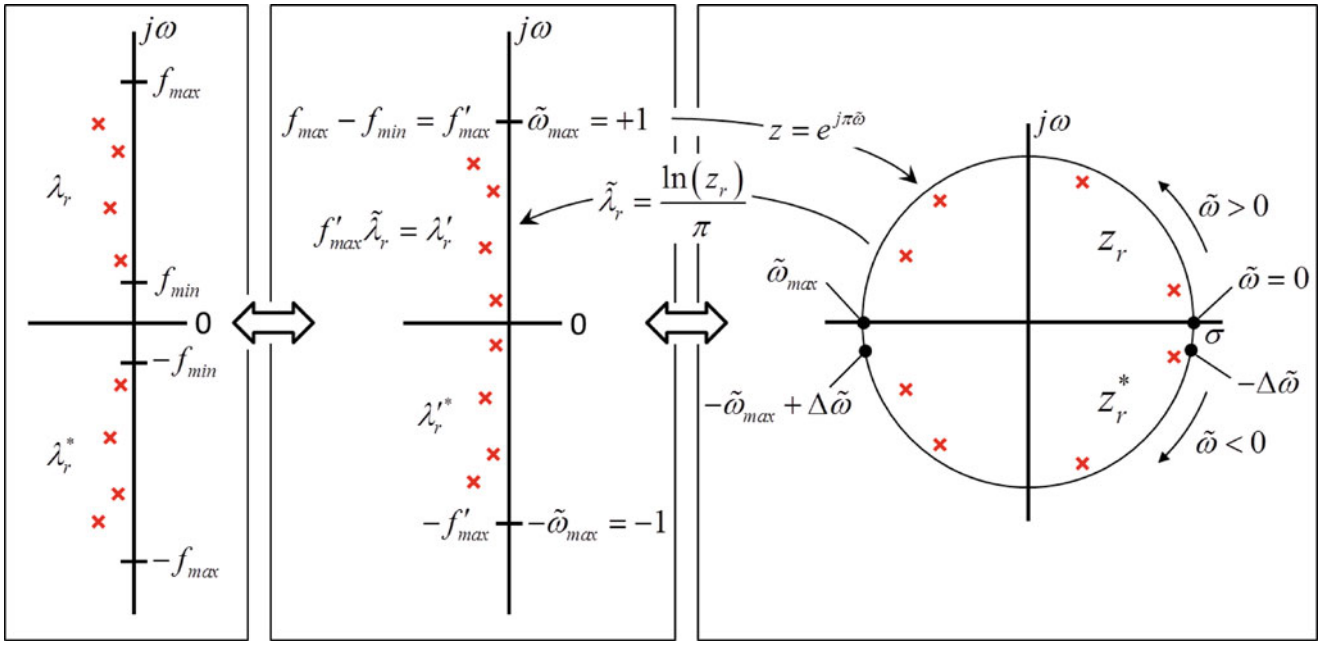


**Fig. 17.3** Frequency mapping for PLSCF as an orthogonal polynomial algorithm

$$\text{where } C = \begin{bmatrix} 0 & I & & 0 \\ 0 & 0 & \ddots & 0 \\ 0 & 0 & & I \\ -\alpha_0 & -\alpha_1 & \cdots & -\alpha_{m-1} \end{bmatrix}, x = \begin{Bmatrix} L_r \\ z_r L_r \\ \vdots \\ z_r^{m-1} L_r \end{Bmatrix}$$

and $L_r$ is the modal participation vector. For the LDOP generalized eigenvalue problem, $W$ is a diagonal matrix of scaling factors and $Q$ is a bi-diagonal matrix of scaled projections. However, since the $z^k$ basis functions are scaled to have unity length, all of the scaling factors are unity and $W = I$, and since the sines and cosines are inherently orthogonal, all the projections are zero and $Q = 0$. The eigenvectors have the customary form of stacked partitions of the modal participation vector multiplied by scalars.

For the formulation that normalizes the characteristic equation with the zeroth-order coefficient $\alpha_0$ as an identity, the eigenvalue problem becomes

$$(I + CQ)\, x = z_r C W x \quad \rightarrow \quad (I + 0)\, x = z_r C I x \quad \rightarrow \quad x = z_r C x \quad \rightarrow \quad z_r^{-1} x = C x, \tag{17.5}$$

$$\text{where } C = \begin{bmatrix} -\alpha_1 & \cdots & -\alpha_{m-1} & -\alpha_m \\ I & & 0 & 0 \\ 0 & \ddots & 0 & 0 \\ 0 & & I & 0 \end{bmatrix}$$

and the eigenvalues as computed are the reciprocal of the z-domain poles.

## 17.6 Characteristic Equation Normalization

Whichever way PLSCF is implemented, it bears the characteristics of the discrete time domain, such as the potential for aliasing. It also inherits another trait that makes a big difference in the "speed" and "clarity" of consistency diagrams: while the algorithm can be formulated for a normalization of the characteristic equation by either the highest- or zeroth-order

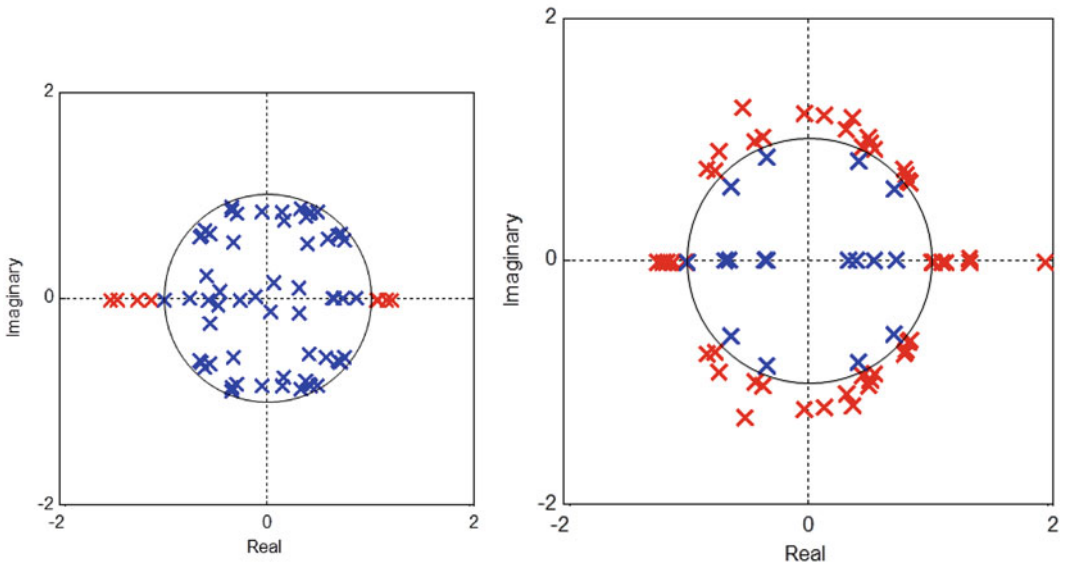


**Fig. 17.4** Z-domain poles for highest-order coefficient normalization (*left*) and zeroth-order coefficient normalization (*right*)

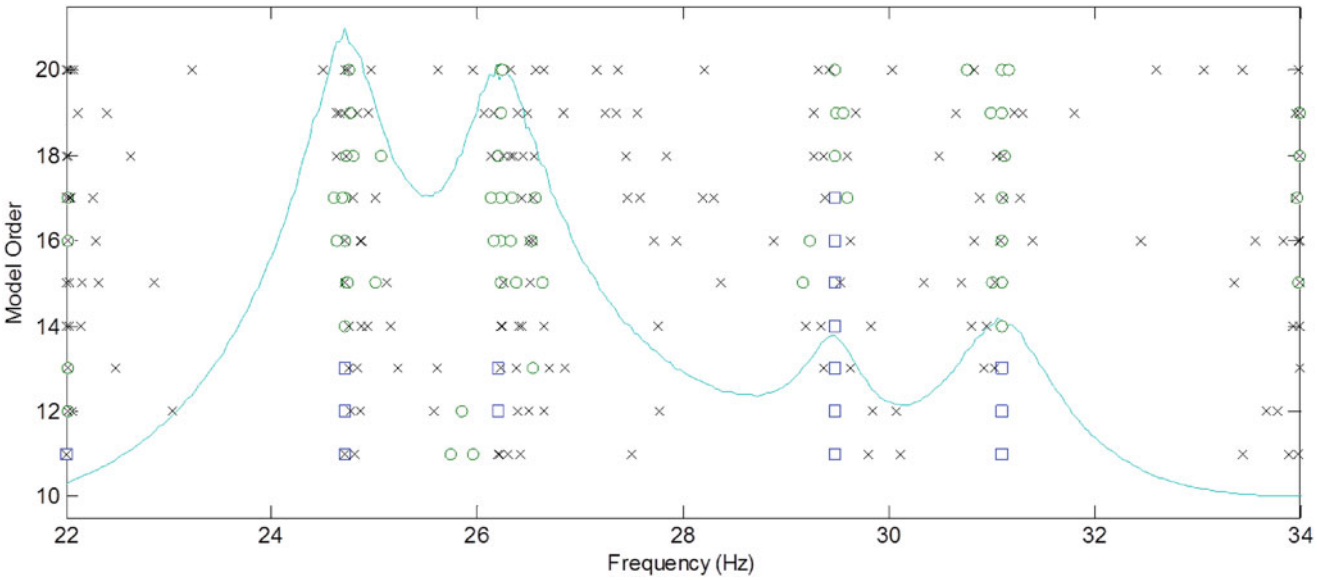


**Fig. 17.5** Consistency diagram for highest-order coefficient normalization

coefficient, it has been shown that in the discrete time domain one choice is decidedly better than the other [7]. The $\alpha_m$ normalization estimates all (or at least most) of the poles as stable (i.e., with a magnitude less than one in the z-domain or with real parts in the left half-plane in the Laplace domain). However, the $\alpha_0$ normalization estimates the consistent, system poles as stable but (almost all of) the computational poles as unstable, and these unstable poles can easily be discarded before assembling the consistency diagram.

In Fig. 17.4 are plotted the z-domain poles for the model order 20 row from the consistency diagrams in Figs. 17.5 and 17.6. The blue x's are the stable poles inside the unit circle, and the red x's are the unstable poles outside the unit circle. There are four modes in the frequency range, and for the $\alpha_0$ normalization only these four poles are inside the unit circle (except for the ones near the real axis, which get pushed to the edges of the frequency range and can usually be ignored). However, for the $\alpha_m$ normalization, there are many more poles inside the unit circle – both the system poles and the computational poles – which leads to a rather messy consistency diagram as shown in Fig. 17.5.

Figure 17.5 is the consistency diagram for the $\alpha_m$ normalization, and Fig. 17.6 is the consistency diagram for the $\alpha_0$ normalization. The green circles are consistent poles (frequency and damping), the blue squares are consistent poles and

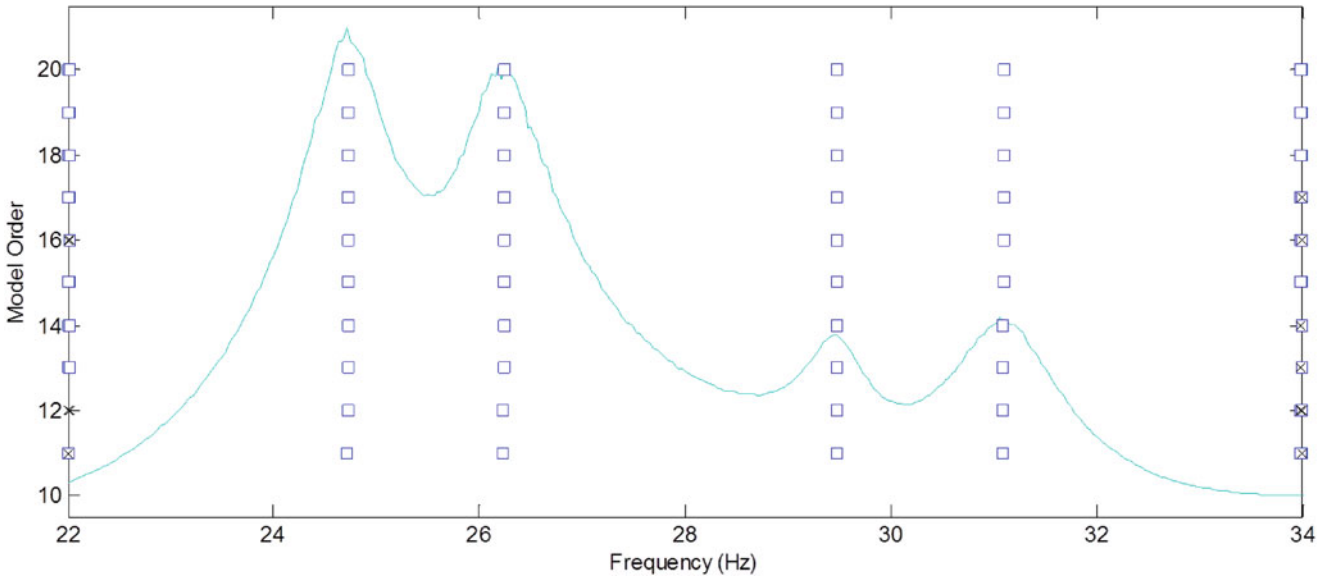


**Fig. 17.6** Consistency diagram for zeroth-order coefficient normalization

vectors (residues), and the black x's are everything else inside the unit circle, as the unstable poles have already been discarded. The only thing that was changed in the processing for these two consistency diagrams was the choice of the coefficient for the characteristic equation normalization – but that made quite a difference.

## 17.7 Uneven Frequency Spacing

There's one small detail that we've overlooked thus far. First consider the consistency diagram in Fig. 17.7, which was generated using the PLSCF method implemented as an orthogonal polynomial algorithm with the recommended $\alpha_0$ normalization. The blue squares indicate consistent poles and vectors, and black x's are everything else inside the unit circle but not too close to the real axis. Most any practitioner of the modal arts would consider this to be a very agreeable outcome. Now consider the consistency diagram in Fig. 17.8, which is the same dataset except that some of the spectral lines between the resonances have been removed. The x-ticks on the consistency diagram indicate the unevenly spaced spectral lines. Something certainly went wrong for the three modes around 500 Hz, and even though some consistent poles were found elsewhere, they are consistently wrong. As shown in the inset of Fig. 17.8, where the squares from the two consistency diagrams are plotted (but not the x's), the damping is too low. What happened here was that while the sines and cosines forming the basis functions are inherently orthogonal when the frequency is evenly spaced, the orthogonality is lost when evaluated at unevenly spaced discrete values.

The uneven frequency spacing in the example given above was meant to simulate a stepped sine test in which the frequency resolution is finer near the resonances and coarser away from the resonances. Although most FRFs are produced via the FFT and have evenly spaced spectral lines, there could be some other occasions in which a dataset intended for modal parameter estimation might have uneven frequency spacing. For example, you might want to exclude a frequency band that is overly noisy or remove harmonics of the electrical line frequency if these are troublesome. Also, if there is a mode that is contaminated by leakage, excluding the spectral lines near the resonance can give a better chance for a reasonable estimate of the pole. As will be shown next, the PLSCF algorithm can be generalized and extended to allow for uneven frequency spacing as well.

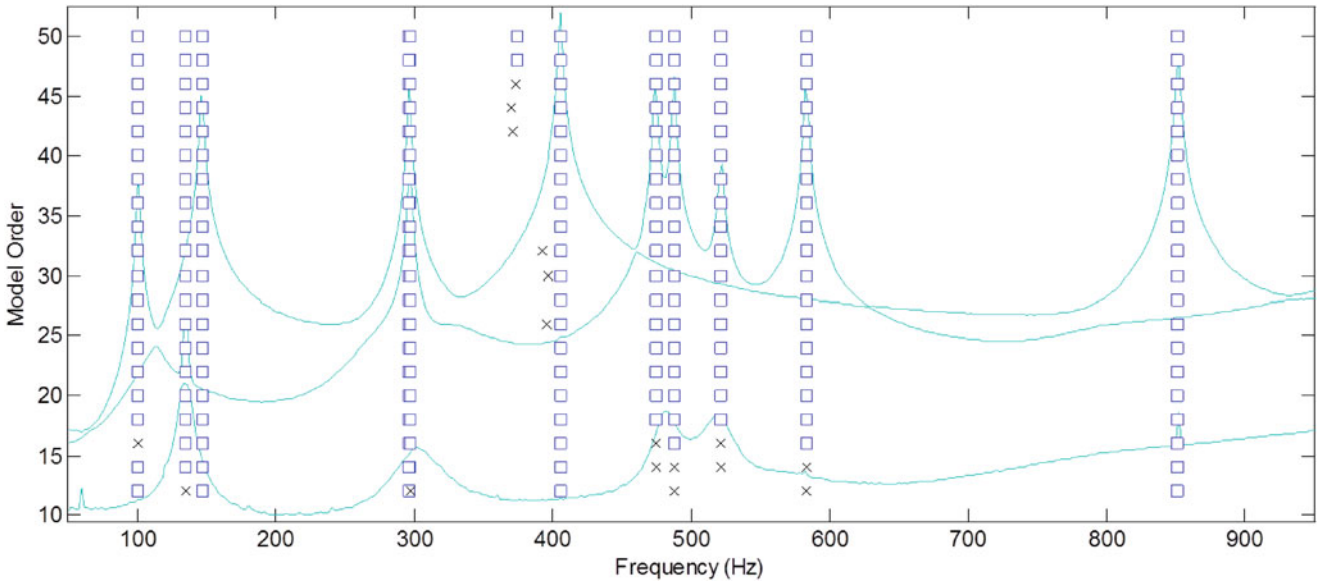


**Fig. 17.7** Consistency diagram for even frequency spacing using trigonometric basis functions

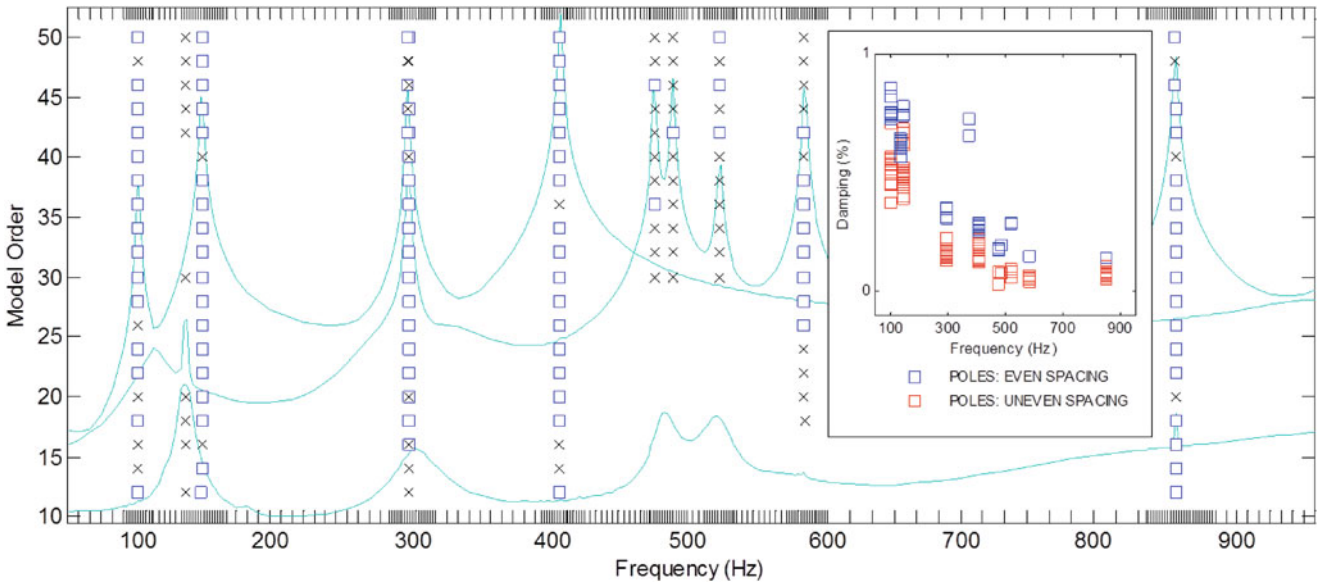


**Fig. 17.8** Consistency diagram for uneven frequency spacing using trigonometric basis functions

## 17.8 The "Reorthogonalized" PLSCF

This limitation of even frequency spacing can be overcome by "reorthogonalizing" the complex polynomial basis functions in the z-domain using the same Gram-Schmidt approach that generates the Laplace-domain orthogonal polynomials. Constructing the orthogonal polynomials for the LDOP algorithm over the interval of $-1$ to $+1$ on the real axis was just one particular choice; they could have been defined over any interval in the complex plane, either on the real axis or on the imaginary axis, or somewhere in between – and it didn't have to be a straight line. So why not the unit circle?

For the Laplace-domain orthogonal polynomials, the frequency range was mapped to the interval of $x \in [-1, +1]$, with no restrictions on the frequency spacing. For the z-domain orthogonal polynomials, the frequency range is shifted and scaled to the interval of $\tilde{\omega} \in [-1, +1]$ and mapped to the unit circle as given in Eq. 17.1, now also with no restrictions on the frequency spacing. Again, the orthogonal polynomials $\xi_k(z_i)$ are constructed recursively, with each successive orthogonal polynomial being one order higher than the preceding one.

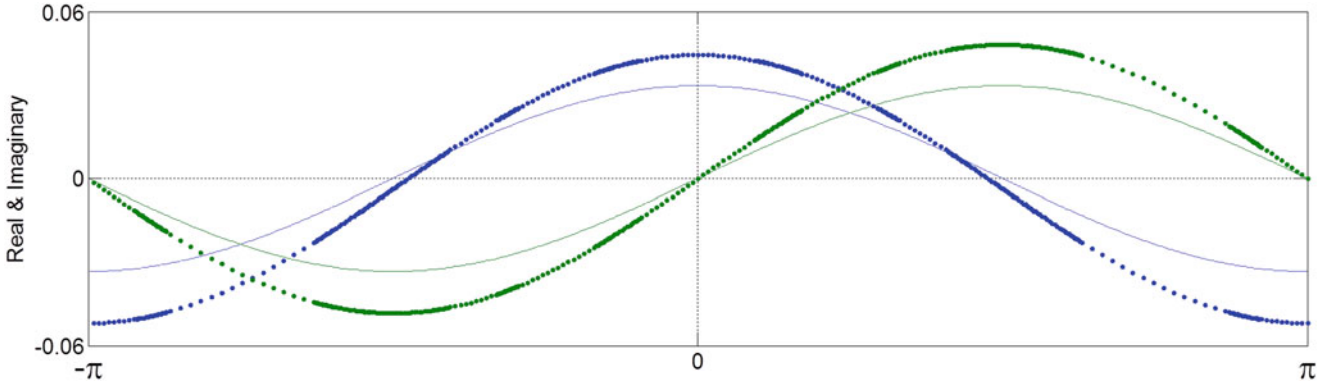


**Fig. 17.9** First-order z-domain basis functions for even and uneven frequency spacing

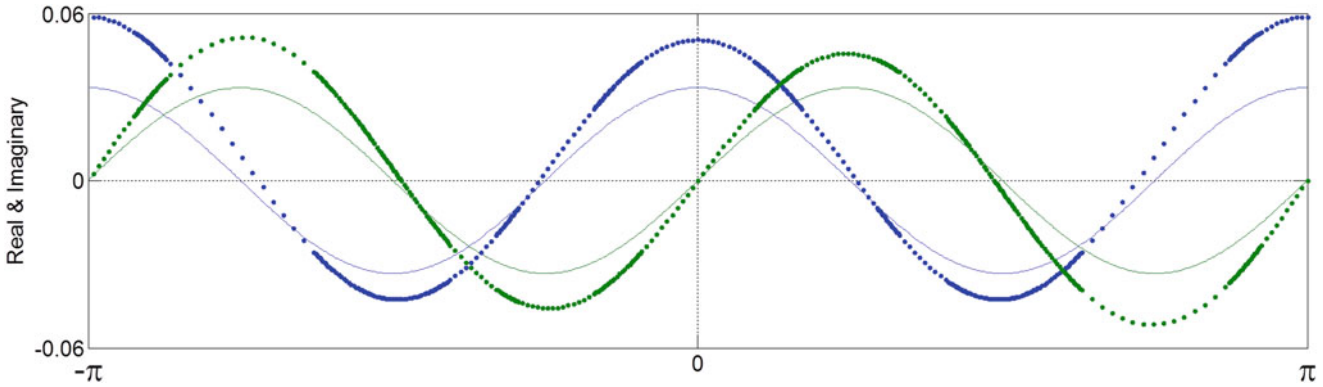


**Fig. 17.10** Second-order z-domain basis functions for even and uneven frequency spacing

The zeroth-order basis function $\xi_0$ is still a real constant normalized to have unity length. Then the higher orders are generated recursively as

$$\xi_k(z_i) = w_k z_i \xi_{k-1}(z_i) - \sum_{n=0}^{k-1} q_{k,n} \xi_n(z_i) \quad \text{for } k \geq 1, \quad \text{where } z_i = e^{j\pi\tilde{\omega}_i}, \tag{17.6}$$

$w_k$ is a scaling factor for unity-length normalization, and $q_{k,n}$ is a scaled projection (i.e., the scalar projection of $\varphi_k$ onto $\varphi_n$ multiplied by $w_k$). Note that there is one slight difference here: while the Laplace-domain orthogonalization required subtracting the projections onto only the preceding two orders, Eq. 17.6 contains the full recurrence from order $k-1$ to 0 [8].

So what do these reorthogonalized basis functions look like and, more importantly, do they have favorable numerical conditioning properties? The zeroth-order polynomial is still a real constant, but the higher orders are more interesting. In Figs. 17.9 and 17.10, the real (blue) and imaginary (green) parts of the first- and second-order polynomials are plotted in dots for the uneven frequency spacing from Fig. 17.8. The thin, solid lines are the trigonometric functions for the even frequency spacing from Fig. 17.7 (real part cosine, blue and imaginary part sine, green). The reorthogonalized functions have the same general pattern as the corresponding cosines and sines; i.e., the first order has one cycle over the interval of $-\pi$ to $\pi$ and the second order has two cycles – they're just reshaped to impose orthogonality with the points over which they are defined.

Figures 17.11 and 17.12 show the real and imaginary parts of orders zero through ten of the reorthogonalized basis functions for the uneven frequency spacing from Fig. 17.8. While the trigonometric functions would have constant amplitude of the interval, these do not. However, they are still nicely bounded.

Figure 17.13 shows the real and imaginary parts of all 51 orders of the reorthogonalized basis functions used to estimate the poles in Fig. 17.14, plotted as dots to accentuate the unevenness of the frequency spacing and show the overall envelope. The condition number of the Vandermonde matrix formed from these polynomials is a perfect one, which means that they will have very favorable numerical conditioning properties. Incidentally, the condition number of the trigonometric basis functions is also unity.

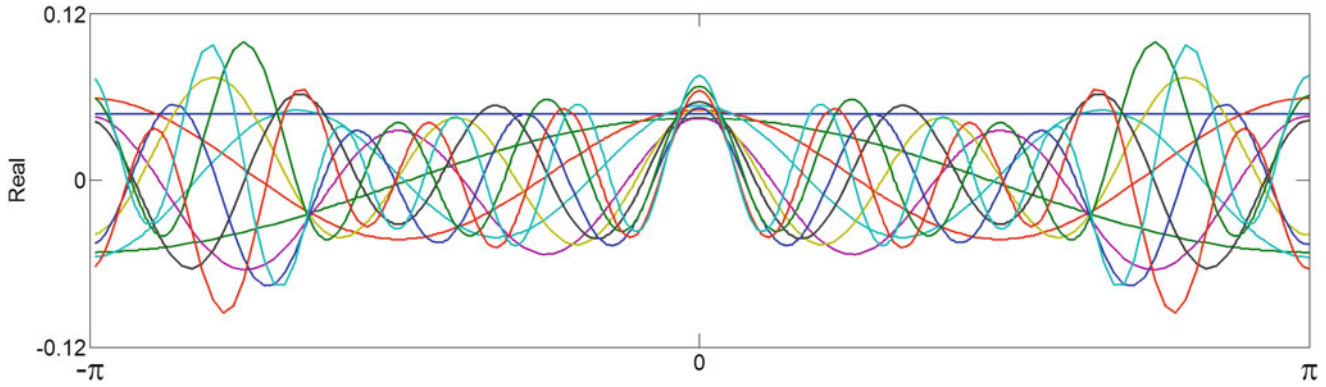


**Fig. 17.11** Real part of orders zero through ten of z-domain basis functions for uneven frequency spacing

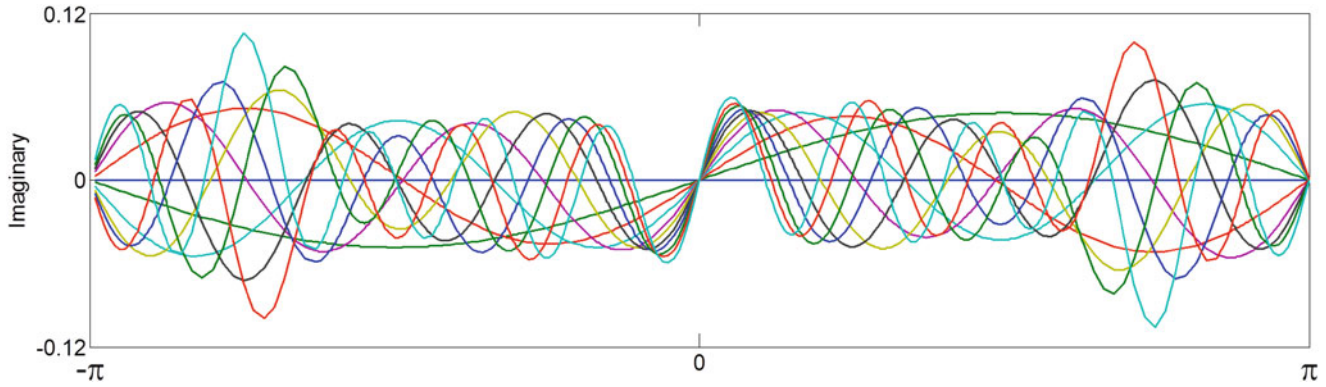


**Fig. 17.12** Imaginary part of orders zero through ten of z-domain basis functions for uneven frequency spacing

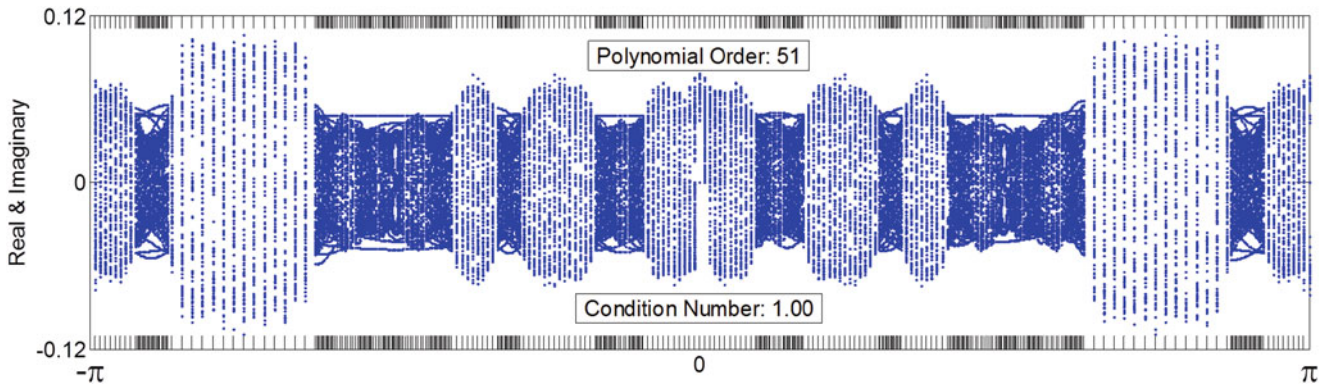


**Fig. 17.13** All 51 orders of z-domain basis functions for uneven frequency spacing

To estimate the poles with these reorthogonalized basis functions, we revert back to the generalized eigenvalue problem formulations for the LDOP algorithm given in Eqs. 17.4 and 17.5. $W$ is the same diagonal matrix of scaling factors $w_k$, but $Q$ is a lower triangular matrix (instead of bi-diagonal) because of the full recurrence for subtracting the scaled projections $q_{k,n}$ in Eq. 17.6.

$$W = \begin{bmatrix} w_1 I & 0 & 0 & 0 \\ 0 & \ddots & 0 & 0 \\ 0 & 0 & \ddots & 0 \\ 0 & 0 & 0 & w_m I \end{bmatrix} \quad \text{and} \quad Q = \begin{bmatrix} q_{1,0} I & 0 & \cdots & 0 \\ q_{2,0} I & q_{2,1} I & \cdots & 0 \\ \vdots & \vdots & \ddots & \vdots \\ q_{m,0} I & q_{m,1} I & \cdots & q_{m,m-1} I \end{bmatrix} \tag{17.7}$$

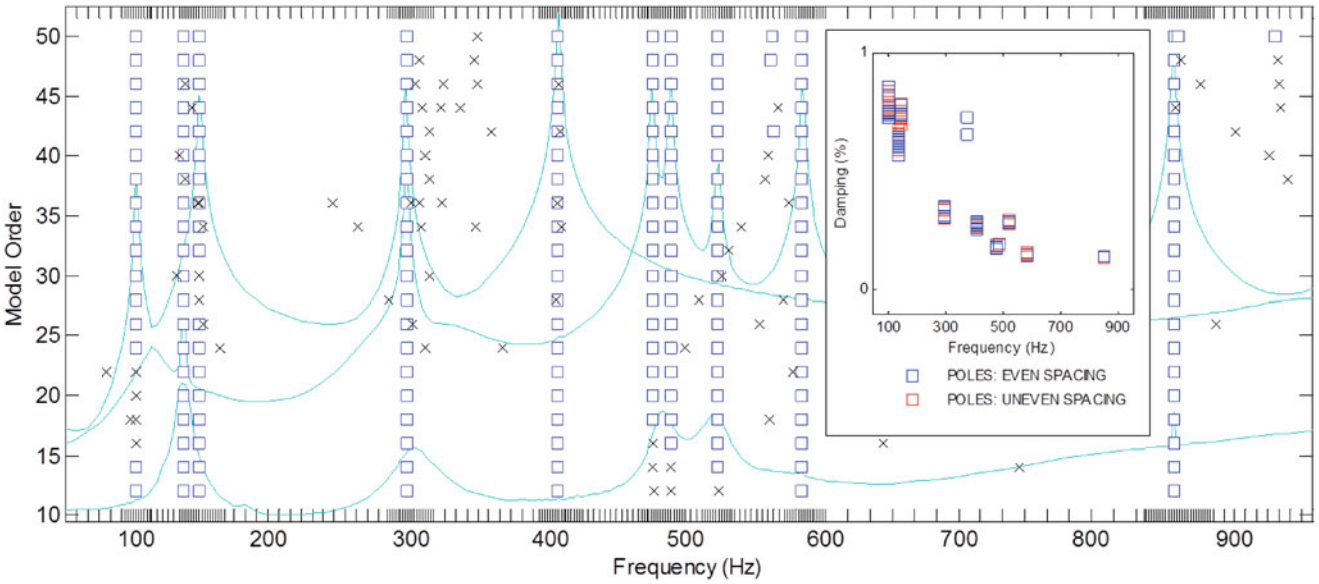


**Fig. 17.14** Consistency diagram for uneven frequency spacing using reorthogonalized basis functions

The results from going to the trouble of creating a set of orthogonal basis functions for the uneven frequency spacing are shown in Fig. 17.14. This consistency diagram looks much better than the one in Fig. 17.8, and we're getting the right answers, too, as shown in the inset. Although it did seem to sprout some more extraneous poles (and there are a few more under the inset), those are not consistent and would not normally be plotted.

## 17.9 A Unified View

In the unified matrix polynomial approach (UMPA), modal parameter estimation algorithms are viewed from a common mathematical framework in order to study their similarities, differences, and numerical characteristics [9]. The underlying high-order model for the methods that process FRFs is based on the rational fraction polynomial model of an FRF.

$$H(j\omega_i) = \frac{\beta_n (s_i)^n + \beta_{n-1}(s_i)^{n-1} + \cdots + \beta_1 s_i + \beta_0}{\alpha_m (s_i)^m + \alpha_{m-1}(s_i)^{m-1} + \cdots + \alpha_1 s_i + \alpha_0} = \frac{\sum_{k=0}^{n} \beta_k (s_i)^k}{\sum_{k=0}^{m} \alpha_k (s_i)^k}, \tag{17.8}$$

where a distinction is made between the measured frequency $\omega_i$ of the FRF and the generalized frequency $s_i$ of the model. To make another level of abstraction, the numerator can be expressed as some generic polynomial $P_\beta$ of the generalized frequency variable, and the denominator can be another generic polynomial $P_\alpha$, also of the generalized frequency variable.

$$H(j\omega_i) = \frac{P_\beta(s_i)}{P_\alpha(s_i)} = \underbrace{\frac{\sum_{k=0}^{n} \tilde{\beta}_k (j\tilde{\omega}_i)^k}{\sum_{k=0}^{m} \tilde{\alpha}_k (j\tilde{\omega}_i)^k}}_{\text{RFP}} = \underbrace{\frac{\sum_{k=0}^{n} \widehat{\beta}_k \varphi_k(x_i)}{\sum_{k=0}^{m} \widehat{\alpha}_k \varphi_k(x_i)}}_{\text{LDOP}} = \underbrace{\frac{\sum_{k=0}^{n} \overline{\beta}_k z_i^k}{\sum_{k=0}^{m} \overline{\alpha}_k z_i^k}}_{\text{PLSCF}} = \underbrace{\frac{\sum_{k=0}^{n} \overline{\beta}'_k \xi_k(z_i)}{\sum_{k=0}^{m} \overline{\alpha}'_k \xi_k(z_i)}}_{\text{ZDOP}} \tag{17.9}$$

The initials under each of the fractions in Eq. 17.9 indicate the modal parameter estimation algorithm represented by that polynomial model. The tildes, hats, bars, and primes on the alphas and betas imply that algorithms will not necessarily produce the same polynomial coefficients and hence will produce different estimates of the poles as well.

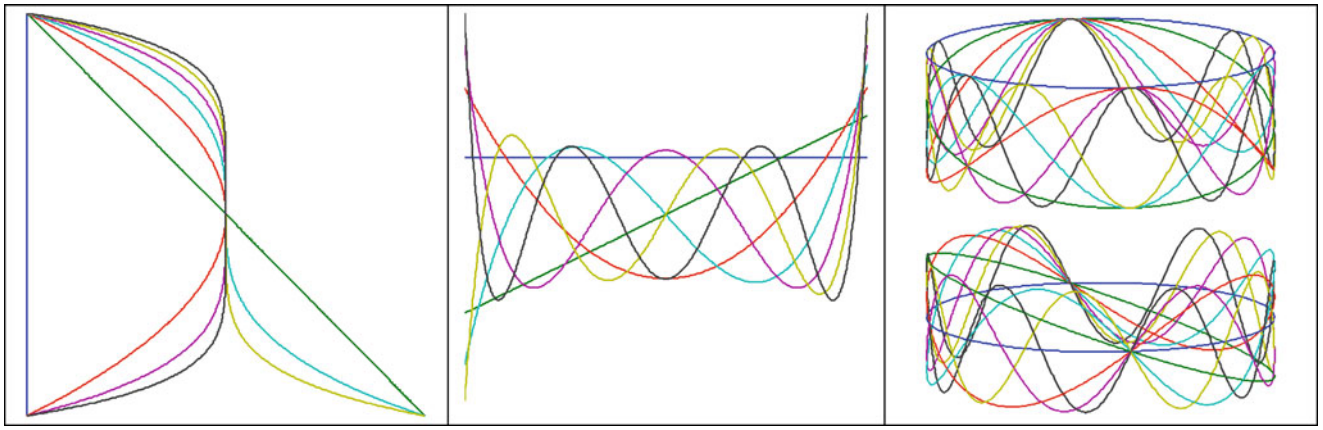

**Fig. 17.15** Basis functions and frequency mapping for RFP (*left*), LDOP (*center*), and PLCSF and ZDOP (*right*)

For RFP, the frequency mapping is just a scaling of the frequency range such that $\tilde{\omega}_i \in [-1, +1]$, and the basis functions are power polynomials of $(j\tilde{\omega}_i)^k$ evaluated over the imaginary axis, as shown in Fig. 17.15 (left). For LDOP, the frequency range is scaled and rotated 90° clockwise to the real axis, and the basis functions are the Laplace-domain orthogonal polynomials $\varphi_k(x_i)$ evaluated over the interval $x_i \in [-1, +1]$, as shown in Fig. 17.15 (center). For PLSCF and ZDOP, the frequency range is shifted, scaled, and mapped from the imaginary axis to the unit circle on the complex plane. If the frequency is evenly spaced, PLSCF uses the trigonometric basis functions $z_i^k$; otherwise ZDOP uses the reorthogonalized basis functions $\xi_k(z_i)$, as shown in Fig. 17.15 (right).

From this point of view, all of these algorithms start from the same place but move to different neighborhoods to do their work. When they're done there, the poles that they produced are then mapped back to reality.

## 17.10 Conclusion

This paper has described how PLSCF can be viewed as the frequency-domain equivalent to PTD or as another version of an orthogonal polynomial algorithm operating a different solution space. From either point of view, it has the traits of a discrete time-domain algorithm and a prevalent choice for the characteristic equation normalization. The method was generalized and extended for uneven frequency spacing by constructing a new set of orthogonal basis functions using a procedure very similar to that used for the traditional Laplace-domain orthogonal polynomials. Although their provenance may differ and their implementations may diverge, all these methods – PLSCF, ZDOP, LDOP, and their ancestor RFP – all fit quite nicely into the UMPA framework – it's just a matter of frequency mapping and basis functions.

## References

1. Richardson M, Formenti DL (1982) Parameter estimation from frequency response measurements using rational fraction polynomials. In: Proceedings of the international modal analysis conference, pp 167–182
2. Fladung W, Vold H (2015) An improved implementation of the orthogonal polynomial modal parameter estimation algorithm using the orthogonal complement. In: Proceedings of the international modal analysis conference, p 16
3. Van der Auweraer H, Guillaume P, Verboven P, Vanlanduit S (2001) Application of a fast-stabilizing frequency domain parameter estimation method. ASME J Dyn Syst Meas Control 123(4):651–658
4. Guillaume P, Verboven P, Vanlanduit S, Van der Auweraer H, Peeters B (2003) A polyreference implementation of the least-squares complex frequency domain estimator. In: Proceedings of the international modal analysis conference, p 12
5. Peeters B, Van der Auweraer H, Guillaume P, Leuridan J (2004) The PolyMAX frequency domain method: a new standard for modal parameter estimation? Shock Vib 11(3–4):395–409
6. Peeters B, Lowet G, Van der Auweraer H, Leuridan J (2004) A new procedure for modal parameter estimation. Sound Vib 5
7. Verboven P, Cauberghe B, Vanlanduit S, Parloo E, Guillaume P (2004) The secret behind clear stabilization diagrams: the influence of the parameter constraint on the stability of the poles. In: Proceedings of the society of experimental mechanics (SEM) annual conference, p 17

8. Rolain Y, Pintelon R, Xu KQ, Vold H (1995) Best conditioned parametric identification of transfer function models in the frequency domain. IEEE Trans Autom Control 40(11):1954–1960
9. Allemang RJ, Phillips AW (2004) The unified matrix polynomial approach to understanding modal parameter estimation: an update. In: Proceedings of the international conference on noise and vibration engineering, p 36